Identification and Characterization of Oxymetazoline Glucuronidation in Human Liver Microsomes: Evidence for the Involvement of UGT1A9

MUKESH K. MAHAJAN,[1,2] VINITA UTTAMSINGH,[3] LIANG-SHANG GAN,[4] BARBARA LEDUC,[2] DAVID A. WILLIAMS[2]

[1]Drug Metabolism and Pharmacokinetics, Immunoinflammation Centre of Excellence in Drug Discovery, GlaxoSmithKline, Collegeville, Pennsylvania

[2]Department of Pharmaceutical Sciences, Massachusetts College of Pharmacy and Health Sciences, Boston, Massachusetts

[3]Drug Metabolism and Pharmacokinetics, Concert Pharmaceuticals, Inc., Lexington, Massachusetts

[4]Drug Metabolism and Pharmacokinetics, Biogen Idec., Inc., Cambridge, Massachusetts

Received 12 April 2010; revised 4 June 2010; accepted 24 June 2010

Published online 28 July 2010 in Wiley Online Library (wileyonlinelibrary.com). DOI 10.1002/jps.22303

ABSTRACT: The incubation of oxymetazoline, a nonprescription nasal decongestant, with human liver microsomes (HLMs) supplemented with uridine-5-diphosphoglucuronic acid (UDPGA) generated glucuronide metabolite as observed by LC/MS/MS. The uridine glucuronosyltransferases (UGTs) responsible for the *O*-glucuronidation of oxymetazoline remain thus far unidentified. The glucuronide formed in HLMs was identified by LC/MS/MS and characterized by one- and two-dimensional NMR to be the β-*O*-glucuronide of oxymetazoline. UGT screening with expressed UGTs identified UGT1A9 as the single UGT isoform catalyzing *O*-glucuronidation of oxymetazoline. Oxymetazoline *O*-glucuronidation by using HLMs was best fitted to the allosteric sigmoidal model. The derived S_{50} and V_{max} values were 2.42 ± 0.40 mM and 8.69 ± 0.58 pmole/(min mg of protein), respectively, and maximum clearance (CL_{max}) was 3.61 L/min/mg. Oxymetazoline *O*-glucuronidation by using expressed UGT1A9 was best fitted to the substrate inhibition model. The derived K_m and V_{max} values were 2.53 ± 1.03 mM and 54.18 ± 16.92 pmole/(min mg of protein), respectively, and intrinsic clearance (CL_{int}) was 21.41 L/(min mg). Our studies indicate that oxymetazoline is not glucuronidated at its nanomolar intranasal dose and thus is eliminated unchanged, because UGT1A9 would only contribute to its elimination at the toxic plasma concentrations. © 2010 Wiley-Liss, Inc. and the American Pharmacists Association J Pharm Sci 100:784–793, 2011

Keywords: oxymetazoline; glucuronosyltransferases (UGTs); enzyme kinetics; phase II metabolism; microsomes; glucuronidation; UGT1A9; liquid chromatography; mass spectrometry

INTRODUCTION

Oxymetazoline (Fig. 1) is a long-acting vasoconstrictor when applied directly on nasal membranes. It has been available as a nonprescription drug in the United States for more than 40 years, having been approved for the relief of nasal congestion from common colds and allergic rhinitis. Nonprescription drug products are often perceived as safe by the consumer because they are freely available for self-medication without a doctor's prescription. Excessive use of oxymetazoline nasal products has contributed to rebound congestion and to cardiovascular and central nervous system adverse events,[1–3] which are indicative of systemic absorption. Although systemic effects have been minimal with recommended intranasal doses of oxymetazoline (daily intranasal dose of 100 μg), a potential risk of systemic absorption and adverse events increases with excessive or overdoses. The estimated incidence of adverse events is very low: 0.14 adverse events per 100,000 patient-years.[4] Although no human metabolism,

Correspondence to: Mukesh K. Mahajan (Telephone: +610-917-5856; Fax: +610-917-4178; E-mail: mukesh.k.mahajan@gsk.com)

Journal of Pharmaceutical Sciences, Vol. 100, 784–793 (2011)

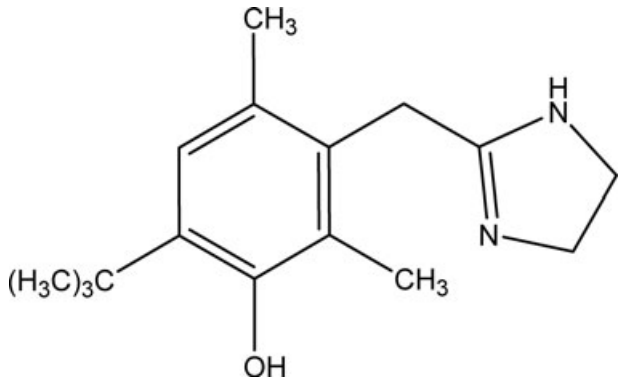

Figure 1. Structure of oxymetazoline.

pharmacokinetic, or toxicological data have been reported thus far for oxymetazoline, the phenolic structure of oxymetazoline suggests *O*-glucuronidation to be its probable detoxification metabolic pathway. What role glucuronide detoxification plays in its low incidence of adverse events and its elimination remains untested. The only intranasal pharmacokinetic study reported for oxymetazoline is the intranasal bioavailability of approximately 7% at 40 μg per rat.[5]

The human uridine glucuronosyltransferases (UGTs) are membrane proteins of the endoplasmic reticulum that are expressed primarily in the liver and are also expressed in extrahepatic tissues, including intestine, lung, kidneys, nasal olfactory epithelium, breast, placenta, testes, and prostate.[6] On the basis of the evolutionary divergence, 28 human UGT genes have been identified and divided into three subfamilies, 1A, 2A, and 2B[7]; however, only 16 of the human UGT genes have been expressed: UGT1A1, UGT1A3, UGT1A4, UGT1A6, UGT1A7, UGT1A8, UGT1A9, UGT1A10, UGT2A1, UGT2A2, UGT2A3, UGT2B4, UGT2B7, UGT2B15, UGT2B17, and UGT2B28.[8]

The identification of specific UGT isoform responsible for metabolism of drugs is critical where glucuronidation has been established as a metabolic pathway. The evaluation of human drug metabolism has been explored by the use of microsomal preparations from human tissue; however, unlike P450 isoforms, the identification of the UGT isoform(s) responsible for glucuronidation of xenobiotics is complicated by overlapping substrate specificity and the lack of specific UGT inhibitors.[9] Emergence of human recombinant cDNA-expressed UGT isoforms expressed in baculovirus-infected insect cells) has made it possible to determine the UGT isoform involved in the glucuronidation of xenobiotics with relatively ease. Therefore, these expressed human UGTs have led to the identification of the UGT isoforms involved in the glucuronidation of a number of phenolic, amino, and carboxylic acid xenobiotics.[10–13]

The objective of the current study was to identify and characterize the glucuronide metabolite of oxymetazoline, to identify the specific UGT isoforms involved in the *in vitro* glucuronidation of oxymetazoline by screening with expressed human UGTs, and to determine the kinetics of oxymetazoline glucuronidation in pooled HLMs and expressed human UGTs. The oxymetazoline glucuronide metabolite was characterized using biosynthetic oxymetazoline glucuronide by one-dimensional (1D) and two-dimensional (2D) NMR as the β-*O*-glucuronide. UGT1A9 was identified as the only UGT isoform catalyzing the β-*O*-glucuronidation of oxymetazoline. The enzyme kinetic experiments were performed by using pooled HLMs and expressed UGT1A9, and their corresponding kinetic parameters were determined.

MATERIALS AND METHODS

Materials

Oxymetazoline, alamethicin, UDPGA (uridine-5-diphosphoglucuronic acid), dimethyl sulfoxide, ammonium formate, monobasic potassium phosphate, and dibasic potassium phosphate were all purchased from Sigma-Aldrich (St. Louis, Missouri). Acetonitrile (HPLC grade) and methanol (HPLC grade) were obtained from Mallinckrodt Baker (Phillipsburg, New Jersey). Magnesium chloride was purchased from Amresco (Solon, Ohio). All other chemicals and reagents were obtained at the highest purity available.

Mixed-gender pooled HLMs ($n = 50$) were obtained from XenoTech, LLC (Kansas City, Kansas). The human recombinant cDNA expressed Supersomes™ (UGT1A1, UGT1A3, UGT1A4, UGT1A6, UGT1A8, UGT1A9, UGT1A10, UGT2B4, UGT2B7, UGT2B15, and UGT2B17) were purchased from BD Gentest (Woburn, Massachusetts). HLMs and expressed UGT enzymes were stored at −80°C and used shortly after receiving them according to the supplier's instructions. The expressed UGT2A enzymes, as well as UGT1A5, UGT1A7, UGT2B10, UGT2B11, and UGT2B28, were not available from BD Gentest for testing. The protein content of all Supersomes™ was 5 mg/mL.

Oxymetazoline Glucuronidation by Pooled HLMs

A 0.1 mM of potassium phosphate buffer solution (pH 7.4) (837.5 μL), containing 3 mM of magnesium chloride and 50 μL of 1 mg of protein/mL of HLMs, was pretreated with 2.5 μL of alamethicin in methanol (50 μg/mg of protein) on ice for 15 min before adding 10 μL of oxymetazoline (50 μM). The incubation tubes were preincubated for 3 min at 37°C in a reciprocal shak ing bath to which 100 μL of UDPGA (5 mM) was added to initiate the reaction.

The reactions were incubated at 37°C in a shaking water bath under ambient oxygenation conditions. The final volume of each incubation was 1000 μL. The reactions were incubated for 60 min to ensure sufficient formation of the glucuronide metabolite. The reactions were terminated at 60 min by the addition of 2 volumes of room temperature acetonitrile to precipitate the protein, and the resulting mixture was chilled at 4°C for 30 min followed by centrifugation at 3000 × *g* to pelletize the protein. The supernatant was collected and dried under a stream of nitrogen in a TurboVap® LV drier (Zymark, Hopkinton, Massachusetts). The dried residues in the tubes were reconstituted in 200 μL of mobile phase (85:15 v/v, 10 mM of ammonium formate, pH 4.0:acetonitrile) in preparation for LC/MS/MS analysis. Incubations of oxymetazoline without UDPGA, drug, or protein were run simultaneously as controls.

An ion trap LC/MS/MS system consisting of an Agilent 1100 HPLC (Agilent Technologies, Palo Alto, California) coupled to a Symmetry C_{18} column (5 μm, 2.1 × 150 mm; Waters Corporation, Milford, Massachusetts) and Finnigan LCQ Deca XP Plus ion trap mass spectrometer (Thermo Fisher Scientific, Inc., Waltham, Massachusetts) was utilized to identify oxymetazoline glucuronide metabolite. The eluant from HPLC column was introduced directly into the mass spectrometer via electrospray ionization in the positive ion mode. The gradient mobile phase consisted of 10 mM of ammonium formate (pH 4.0) as solvent A; solvent B was acetonitrile. The initial mobile phase was 85:15 A/B (v/v) and by linear gradient transitioned to 20:80 A/B (v/v) over 30 min at a flow rate of 0.400 mL/min. Twenty microliters of the reconstituted samples was injected into the equilibrated HPLC. Ionization was assisted with sheath and auxiliary gas (nitrogen) set at 60 and 40 psi, respectively. The electrospray voltage was set at 5 kV, with the heated ion transfer capillary set at 300°C and 30 V. Relative collision energies of 25% to 30% were used when operating in the MS/MS mode of the ion trap.

Oxymetazoline Glucuronidation by Expressed Human UGT Isoforms

Expressed UGT1A1, UGT1A3, UGT1A4, UGT1A6, UGT1A8, UGT1A9, UGT1A10, UGT2B4, UGT2B7, UGT2B15, and UGT2B17 (0.5 mg of protein/mL) incubations were performed and processed in a manner similar to that described for HLMs except that the final volume of each incubation was 500 μL. The incubations were carried out for 30 min to ensure sufficient formation of the glucuronide metabolite, and dried residues were reconstituted in 100 μL of mobile phase. The incubations were performed in duplicate, and the samples were analyzed by the described LC/MS/MS method for pooled HLMs. UGT Control Supersomes™ (0.5 mg of protein/mL) served as the negative control.

Biosynthesis of Oxymetazoline Glucuronide

The oxymetazoline glucuronide was biosynthesized by adding 1250 μL of rabbit liver microsomes (5 mg of protein/mL) and 62.5 μL of alamethicin in methanol (50 μg/mg of protein) to 3137.5 μL of 0.1 mM of potassium phosphate buffer (pH 7.4) containing 3 mM of magnesium chloride in reaction tubes. The tubes were kept on ice for 15 min to which 50 μL of oxymetazoline (100 μM) was added and preincubated for 3 min at 37°C in a reciprocating shaking bath. The final volume of each incubation was 5 mL. The reactions were initiated by the addition of 500 μL of UDPGA (10 mM), incubated at 37°C for 3 h, and terminated after 3 h by precipitating the protein by the addition of 10 mL of acetonitrile to each tube. The tubes were refrigerated at 4°C for 30 min and centrifuged at 3000 × *g* for 10 min to pelletize the protein; the supernatant was collected and dried overnight using the SpeedVac® (Thermo Fisher Scientific Inc.). The gummy residue remaining in each tube was dissolved in 2 mL of mobile phase and sonicated for 2 min, after which the tubes were kept on ice for 30 min. The solution was recentrifuged at 16,000 × *g* for 10 min to pelletize any remaining protein. The supernatant was collected, concentrated using the SpeedVac®, and analyzed for oxymetazoline glucuronide by using the LC/MS/MS method as previously described.

One hundred microliters of injections were made using a Symmetry C_{18} column (5 μm, 2.1 × 150 mm) with the mobile phase and gradient conditions as described previously. The fractions between 4 and 5 min contained the glucuronide and were collected, pooled, and dried overnight using the SpeedVac®. The dried residue was reconstituted in 2 mL of mobile phase and further purified and collected into semipurified fractions by repeated 100-μL LC injections using the same column and mobile phase. Liquid–liquid extraction was then performed using an equal volume of ethyl acetate and the pooled semipurified glucuronide fraction. The glucuronide was back-extracted into the 10 mM of ammonium formate phase (pH 4.0) and all of the other impurities remained in the ethyl acetate phase. Next, solid-phase extraction was performed using a C18 Sep-Pak® cartridge (Waters Corporation) equilibrated with a 50:50 (v/v) acetonitrile:water mixture. The 10 mM of ammonium formate (pH 4.0) phase containing the glucuronide from liquid–liquid extraction was added dropwise to the extraction cartridge and eluted using 90:10 (v/v) of acetonitrile:water. The eluant was collected and dried using the SpeedVac®. Approximately 60 μg of the dried purified glucuronide was recovered. A portion of the dried powder was utilized for LC/MS/MS and NMR analysis, and the

remaining material was stored at −20°C as an authentic standard for quantifying the formation of oxymetazoline glucuronide for kinetic analysis.

Characterization of Oxymetazoline Glucuronide by NMR

^{1}H NMR spectra were acquired on a 600-MHz Varian Inova spectrometer (Varian, Inc., Palo Alto, California) fitted with a Varian 5-mm triple-resonance cold probe. Samples were prepared in DMSO-d_6 at 298.1 K and then transferred into a 5-mm, DMSO-matched Shigemi tube. Chemical shifts are expressed in ppm relative to tetramethylsilane as the internal standard. ROESY (rotating frame nuclear Overhauser effect) experiments were recorded with mixing times of 500 and 750 ms, using a spin-lock field of 4 kHz. A total of 64 complex points were recorded in the F_1 dimension of the correlation plot, with 64 scans acquired per increment. Solvent suppression was achieved by appending the WET pulse-gradient train to the beginning of the ROESY pulse sequence.

Enzyme Kinetics of Oxymetazoline Glucuronidation

The kinetics of oxymetazoline glucuronidation were performed under the same incubation and recovery conditions as previously described for the metabolite identification method, except that the protein concentrations for pooled HLMs were 0.1 and 0.25 mg of protein/mL for expressed UGT1A9. The reactions were incubated for 2.5 min at 37°C for a final volume of 100 μL in 96-well polypropylene plates. The reactions were terminated by the addition of 100 μL of ice-cold acetonitrile containing 1 μM of the internal standard, and the protein-free supernatants were analyzed for the quantification of oxymetazoline glucuronide.

A triple-quadrupole LC/MS/MS system consisting of an Agilent 1100 HPLC, a LEAP autosampler (LEAP Technologies, Carrboro, North Carolina), and a Sciex API 4000 mass spectrometer (Applied Biosystems/MDS Sciex, Foster City, California) was utilized to quantify oxymetazoline glucuronide. Peak area ratios of the oxymetazoline glucuronide and the internal standard (carbutamide) were used to determine the rate of formation of the glucuronide. Separation of the glucuronide was performed on a Phenomenex Synergi™ (Torrance, California) C_{18} Hydro-RP (4 μm; 50 × 3.0 mm) HPLC column. The mobile-phase gradient consisted of 0.1% (v/v) formic acid in water as solvent A; solvent B was 0.1% (v/v) formic acid in acetonitrile. The mobile phase was programmed at a flow rate of 0.5 mL/min, using the following gradient expressed as changes in the mobile phase B: 0 to 1 min, hold at 5% B; 1 to 2.5 min, a linear increase from 5% B to 95% B; and 2.5 to 7 min, a linear decrease from 95% B to 5% B. Oxymetazoline glucuronide and the internal standard were detected by using positive ion spray in the multiple reaction-monitoring mode. The mass transitions monitored were *m/z* 437.2/261.4 for oxymetazoline glucuronide and *m/z* 271.9/155.7 for carbutamide. The mass spectrometer conditions included TurboIonSpray® source temperature of 500°C; nebulizer and desolvation gases set to 60 and 50 psi; and the collision cell gas to 10 (arbitrary units). For all experiments, the spray voltage was set to 5500 V. The declustering potential, entrance potential, collision energy, and collision cell exit potential were optimized at 61, 10, 41, and 6 V, respectively. Analyst software (Version 1.4.1, Applied Biosystems/MDS Sciex, Foster City, CA) was used for data acquisition.

Enzyme Kinetic Data Analysis

All of the data points represent the mean of three separate incubations. The kinetic parameters for oxymetazoline glucuronidation were calculated by fitting the untransformed experimental data to either the single-enzyme Michaelis–Menten model, $v = \{V_{max}[S]\}/\{K_m + [S]\}$, where v is the rate of metabolite formation, V_{max} is the maximum velocity, K_m is the Michaelis constant (substrate concentration at $0.5V_{max}$), and $[S]$ is the substrate concentration; the allosteric sigmoidal (Hill) model,[14] $v = V_{max} \times S^n/(S_{50}^n + S^n)$, where S_{50} is the substrate concentration resulting in 50% V_{max} (analogous to K_m in the Michaelis–Menten equation) and n is the Hill coefficient; or the substrate inhibition model,[15,16] $v = V_{max} \times S/[K_m + S(1 + S/K_{si})]$, where K_{si} is the constant describing the substrate inhibition interaction, using Prism 5.2 (GraphPad, San Diego, California), designed for nonlinear regression analysis. The selection of the "best-fit" kinetic model was based on comparison of the sum-of-squared residuals, standard deviation of fit, coefficient of determination (r^2), and F test (Prism 5.2). Enzyme activity is expressed as reaction rate [pmole/(min mg of protein)].

The intrinsic clearance for the inhibition kinetics ($CL_{int} = V_{max}/K_m$) is expressed as L/(min mg of protein). The maximum clearance for the Hill equation, $CL_{max} = V_{max}\ (n - 1)/\{S_{50} \times n(n - 1)^{1/n}\}$, provides an estimate of the highest clearance attained, that is, when the enzyme is fully activated before saturation occurs.[15]

RESULTS

Oxymetazoline Glucuronidation by HLMs

The mass spectrum of oxymetazoline standard showed a protonated molecular ion $[M + H]^+$ at *m/z* 261 ($C_{16}H_{25}N_2O$) (Fig. 2a). The MS/MS analysis of $[M + H]^+$ at *m/z* 261 (Fig. 2b) yielded product ions at *m/z* 243 (loss of H_2O), *m/z* 205 [neutral loss of 56 amu (C_4H_8, *t*-butyl)], *m/z* 191 [loss of 70 amu from cleavage of the imidazoline ring ($C_3H_6N_2$)], and *m/z* 177

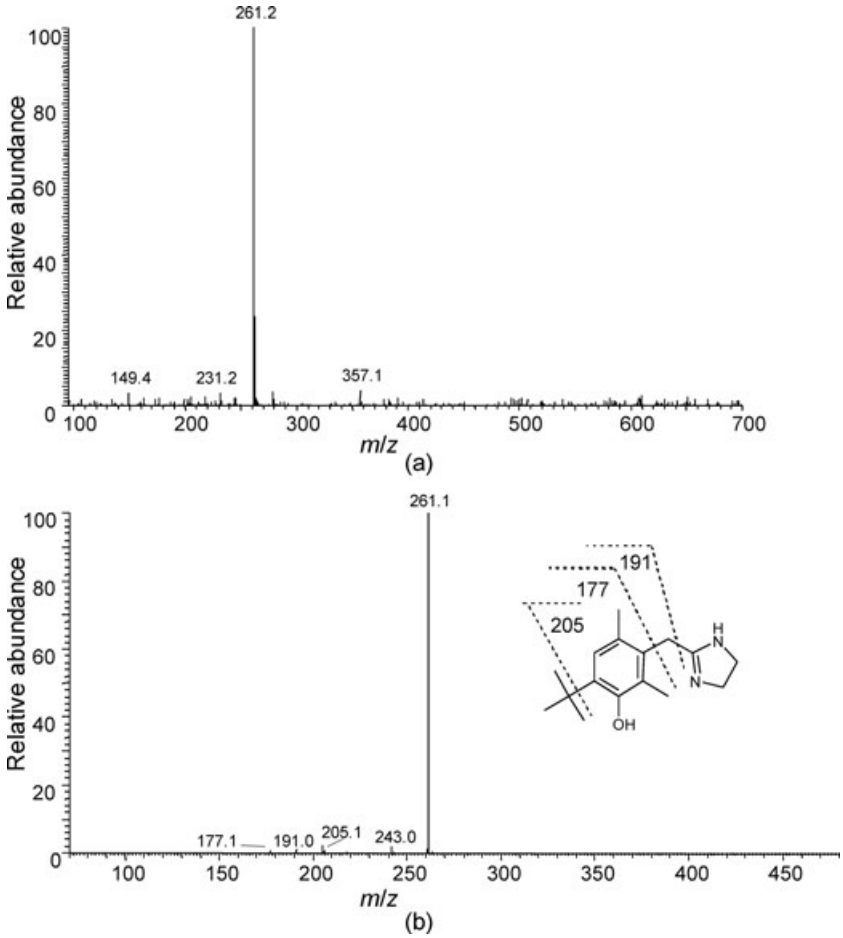

Figure 2. Full mass spectrum (a) and MS/MS spectrum of $[M + H]^+$ at *m/z* 261 (b) for oxymetazoline standard.

[loss of 84 amu from cleavage of the methylimidazoline moiety ($C_4H_8N_2$)]. These four product ion losses are characteristic for oxymetazoline and aid in the identification of oxymetazoline glucuronide metabolite.

While a UV peak was detected at retention time 4.6 min (Fig. 3a) from the incubations containing HLMs supplemented with UDPGA, no peak was observed at the similar retention time from the incubations without UDPGA in HLMs. The extracted ion chromatogram (XIC) for *m/z* 437 (176 amu addition to oxymetazoline) also showed a single peak at 4.8 min (Fig. 3b), further supporting the UV peak at 4.6 min for the formation of oxymetazoline glucuronide. The full mass spectrum showing the $[M + H]^+$ at *m/z* 437 for oxymetazoline glucuronide is shown in Figure 4a. The addition of 176 amu to oxymetazoline indicates the formation of a glucuronide conjugate.[17,18] The MS/MS analysis of $[M + H]^+$ at *m/z* 437 for oxymetazoline glucuronide from HLM incubations gave product ions at *m/z* 261 (characteristic loss of 176 amu for a glucuronide) and *m/z* 205 (loss of 56 amu for *t*-butyl group), which are indicative of an oxymetazoline glucuronide (Fig. 4b). The oxymetazoline glucuronide at retention time 4.6 min was also detected in human liver S9 incubations supplemented with UDPGA having a similar fragmentation pattern as the HLM product at 4.6 min (data not shown).

Oxymetazoline Glucuronidation by Expressed UGT Isoforms

The incubations of oxymetazoline with expressed human UGT isoforms revealed that UGT1A9 is the only UGT catalyzing the glucuronidation of oxymetazoline (Fig. 5). The XIC of the oxymetazoline incubations supplemented with UDPGA and a panel of 11 expressed human UGTs showed a peak at 4.6 min with $[M + H]^+$ at *m/z* 437 for UGT1A9. No XIC glucuronide peak at *m/z* 437 was detected for any of the other UGTs (UGT1A1, UGT1A3, UGT1A4, UGT1A6, UGT1A8, UGT1A10, UGT2B4, UGT2B7, UGT2B15, and UGT2B17). The MS/MS analysis of $[M + H]^+$ at *m/z* 437 gave product ions at *m/z* 261 and *m/z* 205 characteristic for an oxymetazoline glucuronide (data not shown). LC/MS/MS was used to identify the relevant UGT enzymes catalyzing the glucuronidation of oxymetazoline because of its greater sensitivity and selectivity for detecting the glucuronide relative

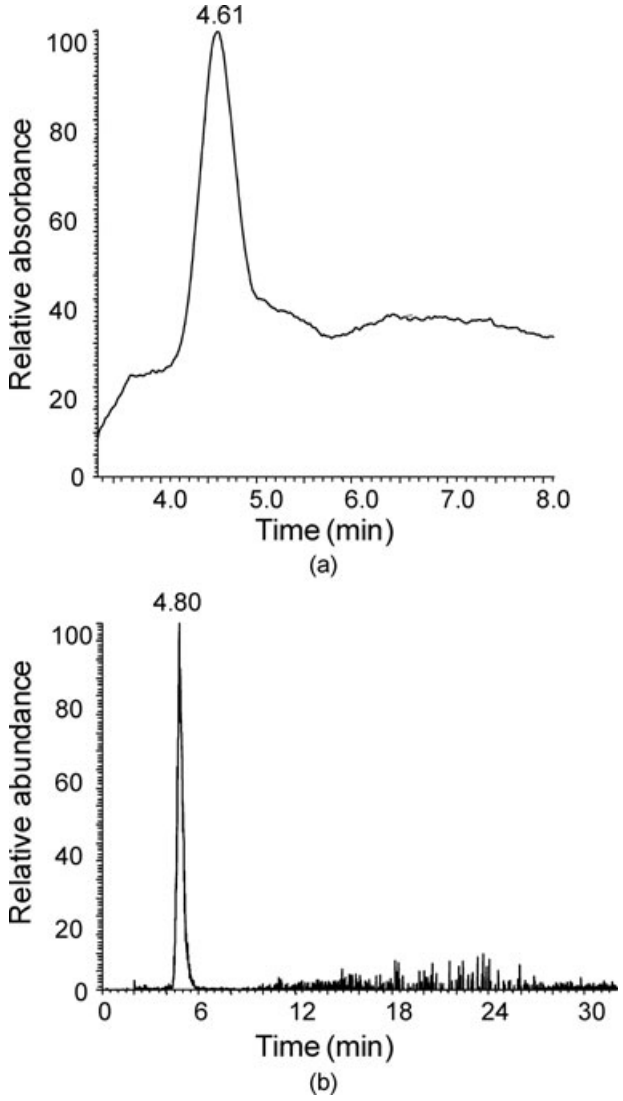

Figure 3. Representative expanded LC–UV chromatogram (a) and extracted ion chromatogram (b) from the oxymetazoline incubations containing alamethicin-activated human liver microsomes supplemented with uridine-5-diphosphoglucuronic acid.

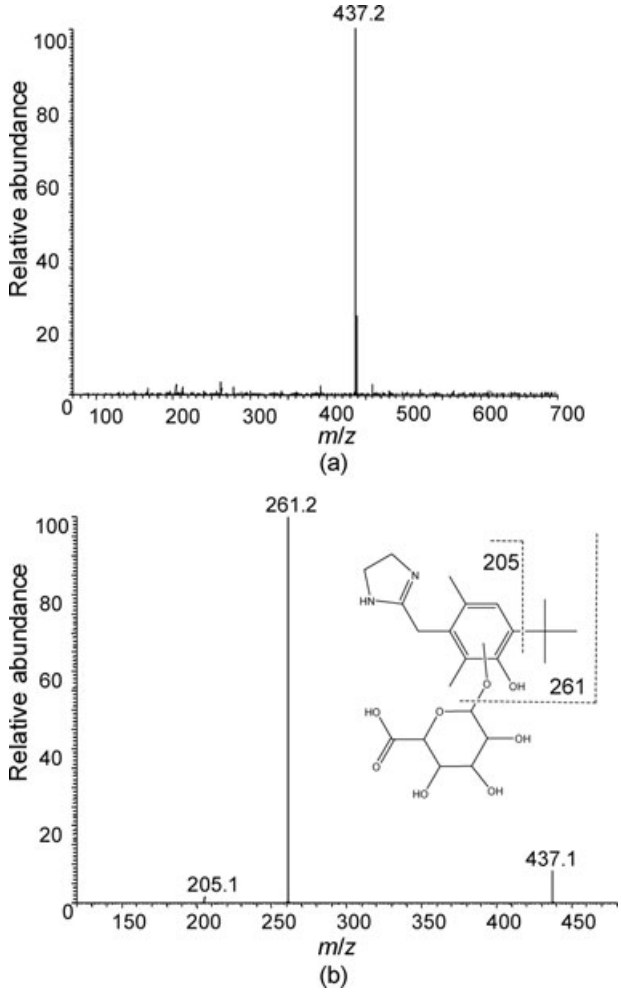

Figure 4. Full mass spectrum (a) and MS/MS spectrum of $[M + H]^+$ at *m/z* 437 (b) from the oxymetazoline incubations containing alamethicin-activated human liver microsomes supplemented with uridine-5-diphosphoglucuronic acid.

to UV detection. These results were used to select UGT1A9 for more detailed kinetic analysis.

Characterization of Oxymetazoline *β*-*O*-Glucuronide by NMR

Because the LC/MS/MS could not identify whether oxymetazoline had been glucuronidated at either the phenolic group or one of the nitrogen atoms of the imidazoline ring, the chemical shift, coupling constants, and integration of the relevant protons in ^{1}H NMR and cross peak interactions of the adjacent protons in 2D-ROESY spectrum of biosynthesized oxymetazoline glucuronide standard were analyzed to characterize the glucuronide as the *O*-glucuronide. The chemical shift and the number of protons integrated for the various peaks of oxymetazoline and oxymetazoline *O*-glucuronide are summarized in Table 1.

Table 1. Comparison of the Chemical Shift of Protons of Oxymetazoline and Oxymetazoline β-*O*-Glucuronide

	Chemical Shift in ppm (# of Integrated Hs)	
Relevant Proton	Oxymetazoline	Oxymetazoline β-*O*-Glucuronide
H_A	1.347 (9 Hs)	1.372 (9 Hs)
H_B	2.107 (3 Hs)	2.170 (3 Hs)
H_C	2.181 (3 Hs)	2.267 (3 Hs)
H_D	3.774 (4 Hs)	3.496 (4 Hs)
H_E	3.858 (2 Hs)	3.585 (2 Hs)
H_F	6.898 (1 H)	6.977 (1 H)
H_1	NA	4.520 (1 H)
H_2	NA	3.088 (1 H)
H_3	NA	2.909 (1 H)
H_4	NA	3.159 (1 H)

NA, not available.

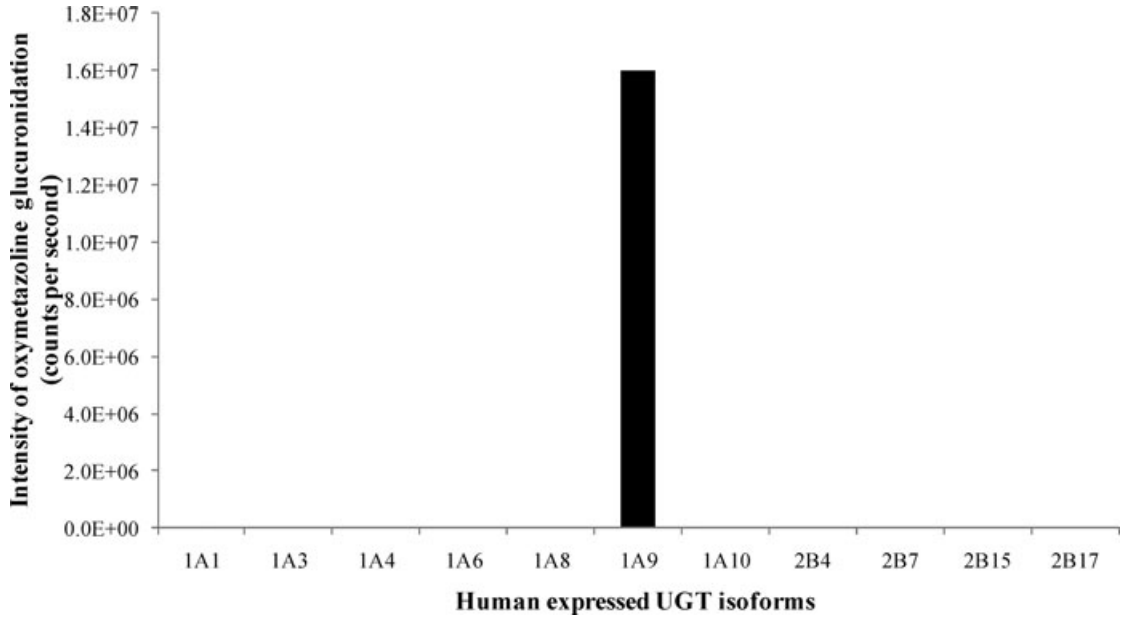

Figure 5. Screening of 11 cDNA expressed human uridine glucuronosyltransferases (UGT) Supersomes™ with 50 μM of oxymetazoline for the formation of oxymetazoline glucuronide. The incubation conditions and extracted-ion LC/MS/MS analysis were as described under the Materials and Methods section. The bar for UGT1A9 represents the mean of duplicate determinations.

The ^{1}H NMR spectrum of the purified oxymetazoline glucuronide standard showed that chemical shift of the anomeric glycosidic proton (H_1) occurs at 4.520 ppm, similar to reports for other *O*-glucuronides.[18,19] Glucuronide proton signals (H_2, H_3, and H_4) were observed at 3.088, 2.909, and 3.159 ppm, respectively.[19] Evidence for the β-*O*-glucuronide was provided by the vicinal trans proton–proton coupling of the anomeric proton H_1 with the H_4 proton of the glucuronide ring. Our results show that the vicinal trans coupling constant for oxymetazoline *O*-glucuronide is 7.751, which is in agreement with the literature values, confirming the β-*O*-glycosidic linkage for oxymetazoline glucuronide.[20,21] Thus, ^{1}H NMR suggests oxymetazoline glucuronide to be the β-*O*-glucuronide.

The attachment of the β-*O*-glucuronide to oxymetazoline was further confirmed with the 2D-ROESY spectrum for the purified oxymetazoline *O*-glucuronide, which showed strong cross peak interactions between the anomeric proton signals (H_1) at 4.520 ppm and the *t*-butyl protons signal (H_A) at 1.372 ppm, the methyl protons (H_C) at 2.267 ppm, the glucuronide proton (H_3) at 2.909 ppm, and the glucuronide proton (H_2) at 3.088 ppm (Fig. 6). Although interactions between H_1 and H_C, H_1 and H_3, and H_1 and H_2 would have been feasible irrespective of the position of glucuronide attachment at a phenolic hydroxyl group or one of the nitrogen atoms of the imidazoline ring, the strong cross peak interaction of *t*-butyl protons (H_A) with the anomeric proton (H_1) indicates that the glucuronide is linked to the phenolic group. Thus, our NMR data utilizing a combination of proton chemical shift assignments, vicinal proton–proton coupling constants, and 2D-ROESY cross peak interactions demonstrate that the oxymetazoline glucuronide formed by pooled HLMs or expressed UGT1A9 is the phenolic β-*O*-glucuronide.

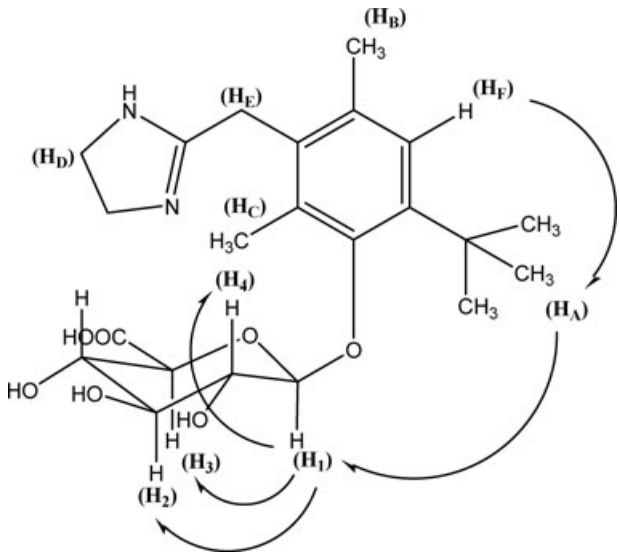

Figure 6. Structure of oxymetazoline β-*O*-glucuronide showing the key two-dimensional (2D) NMR cross peak proton interactions of anomeric proton (H_1) of biosynthesized oxymetazoline β-*O*-glucuronide standard. Samples were prepared in DMSO-d_6 at 298.1 K, and 2D NMR spectra were acquired on 600-MHz Varion Inova spectrometer.

Oxymetazoline *O*-Glucuronidation Kinetics by Pooled HLMs

The initial rate conditions for oxymetazoline glucuronidation with HLMs were determined using a range of protein concentrations (1–4 mg of protein/mL) and incubation times (0–60 min). Oxymetazoline *O*-glucuronidation was determined to be linear up to 2 mg of microsomal protein/mL in HLMs, and the rate of glucuronidation was linear up to 2.5 min.

Oxymetazoline *O*-glucuronidation by pooled HLMs exhibited nonhyperbolic (atypical) kinetics characteristic of allosteric sigmoidal (Hill) kinetics when initially fitted to the Michaelis–Menten equation (Fig. 7a, manifested as a curvilinear Eadie–Hofstee plot inset).[15] Thus, the Hill equation was best fitted to the experimental data, and the derived kinetic parameters by pooled HLMs for S_{50} were 2.42 ± 0.40 mM, V_{max} 8.69 ± 0.58 pmole/(min mg of protein), and Hill coefficient (n) of 1.69, with an apparent CL_{max} of 3.61 L/(min mg of protein). The Hill coefficient is a measure of sigmoidicity.

Oxymetazoline *O*-Glucuronidation Kinetics by Expressed UGT1A9

The initial rate conditions for oxymetazoline *O*-glucuronidation by expressed UGT1A9 were determined in same manner as those for the pooled HLMs. The *O*-glucuronidation of oxymetazoline was determined to be linear up to 1 mg of protein/mL, and the rate of glucuronidation was linear up to 2.5 min with expressed UGT1A9.

In contrast to the sigmoidal kinetics observed by pooled HLMs, oxymetazoline *O*-glucuronidation with expressed UGT1A9 exhibited nonhyperbolic (atypical) kinetics characteristic of substrate inhibition when initially fitted to the Michaelis–Menten equation (Fig. 7b, Eadie–Hofstee plot inset).[15] Thus, the substrate inhibition equation was best fitted to the experimental data and the derived kinetic parameters by UGT1A9 for K_m were 2.53 ± 1.03 mM, V_{max} 54.18 ± 16.92 pmole/(min mg of protein), and k_i 2.44. The apparent CL_{int} (substrate inhibition) was 21.41 L/(min mg of protein). Thus, UGT1A9 appears to exhibit low affinity for oxymetazoline in HLMs.

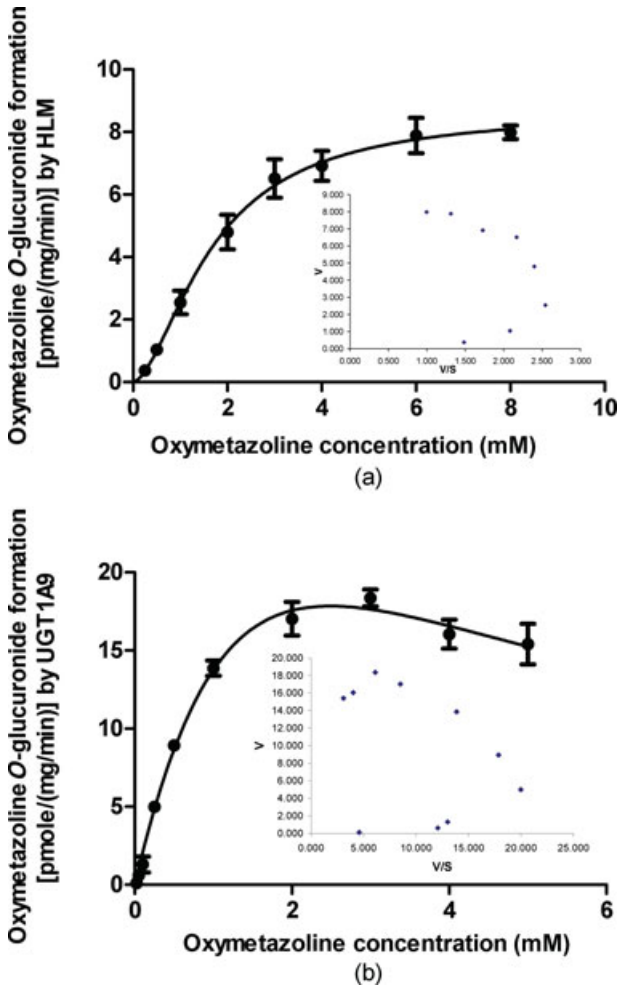

Figure 7. The kinetics of oxymetazoline β-*O*-glucuronidation activity by pooled human liver microsomes (HLMs) represents fitting the Hill equation to the data. The inset shows the curvilinear Eadie–Hofstee plot. The oxymetazoline β-*O*-glucuronidation activity was determined as described under the Materials and Methods section. Each data point represents the mean of triplicate incubations ± SD (a). The kinetics of oxymetazoline *O*-glucuronidation activity by expressed human UGT1A9 from baculovirus-infected insect cells represents fitting the data to the substrate inhibition equation. The inset shows the Eadie–Hofstee plot. The oxymetazoline *O*-glucuronidation activity was determined as described under the Materials and Methods section. Each data point represents the mean of triplicate incubations ± SD (b).

DISCUSSION

The UGT enzymes responsible for catalyzing the glucuronidation of oxymetazoline remain thus far unidentified. Therefore, in this study, we examined the glucuronidation of oxymetazoline by alamethicin-activated pooled HLMs supplemented with UDPGA. The formation of an oxymetazoline glucuronide was identified by LC/MS/MS. The ^{1}H NMR spectrum of this glucuronide showed an anomeric glycosidic proton with a chemical shift and a vicinal proton–proton coupling constant distinctive for the formation of a β-*O*-glucuronide. Thus, the glucuronide was confirmed by NMR to be the β-*O*-glucuronide of oxymetazoline. The 2D-ROESY spectral analysis of cross peak interactions with adjacent protons further confirmed that the phenolic group of oxymetazoline had been *O*-glucuronidated.

Screening with 11 expressed UGTs (UGT1A1, UGT1A3, UGT1A4, UGT1A6, UGT1A8, UGT1A9,

UGT1A10, UGT2B4, UGT2B7, UGT2B15, and UGT2B17) identified UGT1A9 as the only tested isoform catalyzing the *O*-glucuronidation of oxymetazoline. Because no human therapeutic plasma concentrations for oxymetazoline have been reported up to now following intranasal dosing, the 50 μM concentration of substrate, which is at least 130-fold greater than its 380-nM therapeutic dose, was used in the screening study to predict the relative contribution of each isoform to total oxymetazoline glucuronidation.[22] At the 50 μM concentration, no detectable *O*-glucuronidation activities for the other relevant UGTs were observed, suggesting that the other enzymes are unlikely to participate in the *in vitroO*-glucuronidation at purportedly subnanomolar therapeutic plasma concentrations.

The kinetics for the *O*-glucuronidation of oxymetazoline was assessed by alamethicin-activated pooled HLMs and expressed UGT1A9 supplemented with UDPGA. A limitation for this study was the lack of human nasal epithelia–expressed UGT2A1 and UGT2A2 to also assess the *O*-glucuronidation of oxymetazoline. The *O*-glucuronidation of oxymetazoline by pooled HLMs exhibited allosteric sigmoidal (Hill) kinetics, whereas expressed UGT1A9 showed substrate inhibition kinetics. Because pooled HLMs are a crude mixture, it contains many artifactual substances that could contribute to sigmoidicity of the observed HLM kinetics.[15] The value of K_m from the results with expressed enzyme indicates UGT1A9 to be a low-affinity enzyme and thus glucuronidates oxymetazoline with poor efficiency at the subnanomolar therapeutic plasma concentrations anticipated from a 380-nM intranasal dose. A substrate that is glucuronidated solely by a single expressed UGT isoform should have an apparent K_m similar to the apparent K_m for pooled HLMs, which was observed for oxymetazoline, confirming the results from the screening study. The *in vitro* clearance of oxymetazoline was assessed as CL_{int} (substrate inhibition kinetics) for expressed UGT1A9 or CL_{max} (sigmoidal Hill kinetics) for pooled HLMs. CL_{max} provides an estimate of the highest clearance attained prior to saturation of the enzyme active sites. When the kinetic parameters for oxymetazoline are compared with the reported values for the sterically hindered and structurally similar *O*- diisopropylphenol, propofol (K_m = 45 μM), oxymetazoline exhibits approximately 50-fold less affinity and 40-fold less reactivity for UGT1A9 and Cl_{int} is 2.5-fold less than that for propofol [Cl_{int} 54.3 L/(min mg of protein)].[23] These results would seem to indicate that the low affinity for oxymetazoline is not likely due to steric hindrance of the phenolic group by the flanking *t*-butyl and methyl groups but to other factors. Thus, because the value of K_m for glucuronidation of oxymetazoline by UGT1A9 is more than 6000-fold than its intranasal therapeutic dose, the drug would be eliminated unchanged.

In conclusion, the β-*O*-glucuronide of oxymetazoline has been identified as the only glucuronide formed by pooled HLMs and expressed UGT1A9 and was detected by LC/MS/MS and characterized by 1D and 2D NMR. Screening with 11 expressed human UGT isoforms identified UGT1A9 as the only detectable UGT catalyzing the β-*O*-glucuronidation of oxymetazoline by HLMs. From a clinical perspective, our results show that the low incidence of adverse events for oxymetazoline at its therapeutic dose cannot be attributed solely to its elimination via the glucuronide detoxification pathway, because UGT1A9 would contribute only to its elimination at toxic plasma concentrations. This study highlights the fact that the identification and the kinetics of the UGT isoform are crucial to a thorough understanding of human drug disposition and safety.

ACKNOWLEDGMENTS

The authors thank Drs Chuang Lu, Scott Daniels, Ian Parsons, Ajit Chavan, and Sandeep Pusalkar for their assistance and helpful discussions.

REFERENCES

1. Thrush DN. 1995. Cardiac arrest after oxymetazoline nasal spray. J Clin Anesth 7:512–514.
2. Soderman P, Sahlberg D, Wiholm BE. 1984. CNS reactions to nose drops in small children. Lancet 323:573.
3. Glazener F, Blake K, Gradman M. 1983. Bradycardia, hypotension, and near-syncope associated with Afrin (oxymetazoline) nasal spray. N Engl J Med 309:731.
4. Savage R. 2009. Safety of bromhexine and topical nasal decongestants presentation 18 August 2009. Accessed February 24, 2010, at: http://www.medsafe.govt.nz/hot/alerts/CoughandCold/Safety Bromhexine.pdf.
5. Hayes FJ, Baker TR, Dobson RLM, Tsueda MS. 1995. Rapid liquid chromatographic-mass spectrometric assay for oxymetazoline in whole rat blood. J Chromatogr A 692:73–81.
6. Sneitz N, Court MH, Zhang X, Laajanen K, Yee KK, Dalton P, Ding X, Finel M. 2009. Human UDP-glucuronosyltransferase UGT2A2: cDNA construction, expression, and functional characterization in comparison with UGT2A1 and UGT2A3. Pharmacogenet Genom 19:923–934.
7. Mackenzie PI, Owens IS, Burchell B, Bock KW, Bairoch A, Bélanger A, Fournel-Gigleux S, Green M, Hum DW, Iyanagi T, Lancet D, Louisot P, Magdalou J, Chowdhury JR, Ritter JK, Schachter H, Tephly TR, Tipton KE, Nebert DW. 1997. The UDP-glycosyltransferase gene superfamily: Recommended nomenclature update based on evolutionary divergence. Pharmacogenetics 7:255–269.
8. Stone AN, Mackenzie PI, Galetin A, Houston JB, Miners JO. 2003. Isoform selectivity and kinetics of morphine 3- and 6-glucuronidation by human UDP-glucuronosyltransferases: Evidence for atypical glucuronidation kinetics by UGT2B7. Drug Metab Dispos 31:1086–1089.
9. Miners JO, Smith PA, Sorich MJ, McKinnon RA, Mackenzie PI. 2004. Predicting human drug glucuronidation parameters: Application of *in vitro* and *in silico* modeling approaches. Annu Rev Pharmacol Toxicol 44:1–25.

10. Court MH, Duan SX, Von Moltke LV, Greenblatt DJ, Patten CJ, Miners JO, Mackenzie PI. 2001. Interindividual variability in acetaminophen glucuronidation by human liver microsomes: Identification of relevant acetaminophen UDP-glucuronosyltransferase isoforms. J Pharmacol Exp Ther 299:998–1006.
11. Nakajima M, Sakata N, Ohashi N, Kume T, Yokoi T. 2002. Involvement of multiple UDP-glucuronosyltransferase 1A isoforms in glucuronidation of 5-(4′-hydroxyphenyl)-5-phenylhydantoin in human liver microsomes. Drug Metab Dispos 30:1250–1256.
12. Watanabe Y, Nakazima M, Ohashi N, Kume T, Yokoi T. 2003. Glucuronidation of etoposide in human liver microsomes is specifically catalyzed by UDP-glucuronosyltransferase 1A1. Drug Metab Dispos 31:589–595.
13. Zhang JY, Zhan J, Cook CS, Ings RM, Breau AP. 2003. Involvement of human UGT2B7 and 2B15 in rofecoxib metabolism. Drug Metab Dispos 31:652–658.
14. Weiss JN. 1997. The Hill equation revisited: Uses and misuses. FASEB J 11:835–841.
15. Houston JB, Kenworthy KE. 2000. *In vitro–in vivo* scaling of CYP kinetic data not consistent with the classical Michaelis—Menten model. Drug Metab Dispos 28:246–254.
16. Venkatakrishnan K, Von Moltke LL, Greenblatt DJ. 2001. Human drug metabolism and the cytochromes P450: Application and relevance of *in vitro* models. J Clin Pharmacol 41:1149–1179.
17. Mutlib AE, Abbott FS. 1992. Isolation and characterization of carbinolamide and phenolic glucuronide conjugates of (+−)-*N*-methyl-*N*-(1-methyl-3,3-diphenylpropyl) formamide and *N*-formylmethamphetamine by FAB/MS, LC/MS/MS, and NMR. Drug Metab Dispos 20:451–460.
18. Mutlib AE, Chen H, Nemeth GA, Markwalder JA, Seitz SP, Gan LS, Christ DD. 1999. Identification and characterization of Efavirenz metabolites by liquid chromatography/mass spectrometry and high field NMR: Species differences in the metabolism of Efavirenz. Drug Metab Dispos 27:1319–1333.
19. Krishnaswamy S, Duan SX, Moltke VLL, Greenblatt DJ, Sudmeier JL, Bachovchin WW, Court MH. 2003. Serotonin (5-hydroxytryptamine) glucuronidation *in vitro*: Assay development, human liver microsome activities and species differences. Xenobiotica 33:169–180.
20. Matsui M, Okada M, Ishidate M. 1969. Studies on the glucaric acid pathway in the metabolism of d-glucuronic acid in mammals, part II. Excretion of d-glucaric acid in urine after administration of several monosaccharides and their derivatives to mammals. Chem Pharm Bull 17:1064–1071.
21. Oatis JE Jr, Baker JP, McCarthy D, Knapp DR. 1983. Synthesis and chromatographic separation of the glucuronides of (*R*)-and (*S*)-propranolol. J Med Chem 26:1687–1691.
22. Ogilvie BW, Usuki E, Burton A, Yerino P, Parkinson A. 2008. *In vitro* approaches for studying the inhibition of drug-metabolizing enzymes and identifying the drug-metabolizing enzymes responsible for the metabolism of drugs (reaction phenotyping) with emphasis on cytochrome P450. In Drug–drug interactions; Rodrigues AD, Ed. 2nd ed. New York: Marcel Dekker Inc., pp 231–258.
23. Soars MG, Ring BJ, Wrighton SA. 2003. The effect of incubation conditions on the enzyme kinetics of UDP-glucuronosyltransferases. Drug Metab Dispos 31:762–767.